

# Reconstructed respiration and cardio-respiratory phase synchronization in post-infarction patients

Aicko Y. Schumann, Anja Kuhnhold, Katharina Fuchs, Ronny P. Bartsch, Axel Bauer, Georg Schmidt, and Jan W. Kantelhardt

**Abstract**—Cardio-respiratory phase synchronization has been studied in healthy subjects for several years, but little is known about how cardiovascular impairments affect this subtle phenomenon. In this paper we study data from 874 post-infarction patients, where heartbeat intervals and respiration were recorded approximately one week after the index myocardial infarction event. Calculating the intensity of the first Fourier mode of the cyclic relative phase differences we find that cardio-respiratory phase synchronization is decreased in patients with increased mortality risk or age. However, our analysis also indicates that data from 30 minutes recordings is insufficient to achieve a reliable statistics for predicting mortality risk based on phase synchronization. Therefore, we further develop techniques for extracting respiratory information from ECG recordings to be able to use long-term Holter recordings of post-infarction patients in future studies. We compare breathing-phase reconstructions based on the amplitude of the R peaks in the ECG or beat-to-beat time intervals with real respiratory phases. We find that the reconstruction works better for R peak amplitudes in most patients. We optimize the respiration-reconstruction algorithm and show that it works well for a large group of the patients in our database.

**Index Terms**—heart rate, respiration, phase synchronization, first Fourier mode, reconstruction, post-infarction patients, mortality risk

## I. INTRODUCTION

The chances to die of a sudden cardiac death (SCD) are particularly high after an acute myocardial infarction [1], [2]. In fact SCD is among the major causes of deaths in the industrialized world [3]–[5]. Studies in high-risk survivors have reported a reduced mortality due to the implantation of an implantable cardioverter defibrillator (ICD) device [6], [7]. Thus, the identification of post-infarction patients at risk of SCD is a crucial element in post-infarction therapy and surgery. Besides the currently used gold standard for mortality-risk assessment, left ventricular ejection fraction (LVEF) [8], several other predictors and scores have been suggested. For instance, the number of ventricular premature beats (VPBs) per hour [9], various time domain and spectral measures of heart rate variability (HRV) [10], or deceleration capacity (DC)

describing the heart’s capability to decelerate [11], [12] have been proven to be subsidiary (VPBs) or superior predictors. Other studies associated cases of congestive heart failure (CHF) with a general loss in fractal structure and complexity manifesting itself in a reduced short-term scaling exponent [13], [14] which was proven to possess a strong predictive power of mortality in post-infarction patients [15]–[17]. A very recent study utilized a reduced respiratory sinus arrhythmia (RSA) among high risk patients for risk assessment [18].

RSA, that is a modulation of heart rate due to respiration [19]–[21], is strongly related to a phenomenon known in physics as synchronization. Respiration influences the sympathovagal balance of the autonomous nervous system and, thus, affects heartbeat. While a sympathetic predominance during inspiration causes the heart to accelerate (shorter beat-to-beat intervals), expiration suppresses sympathetic output and enhances vagal tone yielding a reduction in heart rate, i.e., a prolongation in beat-to-beat intervals.

In the concept of nonlinear dynamics synchronization is understood as an adjustment of rhythms observed in coupled oscillators due to a (sufficiently weak) interaction with each other [22]. A particular feature of oscillators in synchrony is phase-synchronization (PS) which has been quantified and measured by mutual information [23], studying the Shannon entropy of the signals [24], conditional phase relationships [24], synchrograms [21], [25]–[28], or by calculating the first Fourier mode of both signal’s phase differences [29].

In this paper we reconstruct respiration in two different ways and study, firstly, how reliably such reconstruction can be used as a proxy for real respiration, secondly, tackle the question to which extent cardio-respiratory phase-synchronization can be studied using heartbeat and respiration reconstructed from heartbeat, and finally, discuss the usability of phase-synchronization for mortality-risk assessment.

## II. DATA AND METHODS

### A. Measurements and Preprocessing

From 874 survivors of an acute myocardial infarction 3-lead high-resolution electrocardiogram (1600Hz), blood pressure, and thorax excursion were recorded simultaneously for 30 minutes. All recordings were obtained within the second week after the index infarction event, in supine position, and under resting conditions. For measuring ECG signals we used the orthogonal bipolar Frank-leads X (right mid-auxillary line (I) ↔ left mid-auxillary line (A)), Y (neck (H) ↔ left lower leg (F)), and Z (center of sternum (E) ↔ above vertebral column (M)). Thorax excursion was monitored by stretch sensors incorporated in an elastic belt around the thorax.

A.Y.S. is with the Complexity Science Group at the Department of Physics and Astronomy, University of Calgary, Canada, email: ay.schumann@ucalgary.ca

A.K., K.F. and J.W.K. are with the Institute of Physics, Martin-Luther-University Halle-Wittenberg, 06099 Halle, Germany, email: jan.kantelhardt@physik.uni-halle.de

R.P.B. is with Harvard Medical School and Division of Sleep Medicine, Brigham and Women’s Hospital, Boston, USA

A.B. is with Innere Medizin III - Kardiologie, Eberhard-Karls-University Tübingen, Germany

G.S. is with the 1. Medizinische Klinik, Technical University Munich, Germany

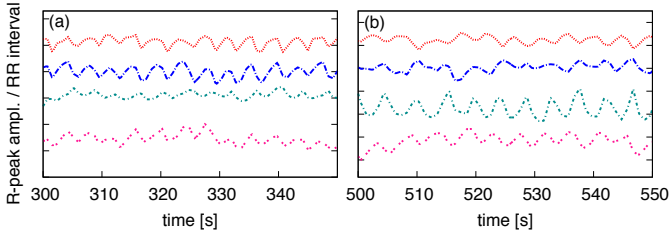


Fig. 1. R-peak amplitudes and R-R intervals from ECG signals recorded from post-infarction patients at times where the best respiration reconstruction is obtained from (a) amplitudes and (b) intervals; from top to bottom: Frank-leads X (red), Y (blue), and Z (turquoise), as well as the RRI signal (pink).

ECG data was preprocessed using the QRS-complex detection software Librasch [30]. Identified heartbeats and their classification, i. e., normal beat, ectopic beat, or artifact, were checked by trained personnel. We consider the times  $t_k, k = 1, \dots, N$  of R peaks (depolarization of ventricles) as a proxy for heartbeat times and derive the signal of beat-to-beat time intervals (RRI) from the ECG-lead containing the least artifacts. While we keep ventricular and super-ventricular beats, artifacts are excluded from the analysis. In addition we calculate the amplitudes of the R peaks from all three leads. Figure 1 shows two typical examples of the data derived from ECGs. Finally, all five time series (three R-peak signals, RRI, and thorax excursion as proxy of real respiration) are resampled to 4Hz by a linear interpolation of the values.

### B. Calculation of Respiratory Phase Signals

In order to obtain a phase signal for the real-respiration recording,  $x(t)$ , we employ the analytical signal approach by complementing  $x(t)$  with its complex counterpart  $i\tilde{x}(t)$  that is defined via a Hilbert transform [31], [32]

$$\tilde{x}(t) = \frac{1}{\pi} \text{P.V.} \int_{-\infty}^{\infty} \frac{x(t')}{t-t'} dt'. \quad (1)$$

Here, P.V. denotes the Cauchy principal value. From the analytical signal expression

$$\hat{x}(t) = x(t) + i\tilde{x}(t) = A(t)e^{i\varphi(t)} \quad (2)$$

follow both the instantaneous amplitude signal,  $A(t) = \sqrt{x^2(t) + \tilde{x}^2(t)}$ , and the instantaneous phase signal,  $\varphi(t) = \tan^{-1}\{\tilde{x}(t)/x(t)\}$ . The Hilbert transform in Eq. (1) requires two prerequisites in order to result in meaningful amplitude and phase signals: (i) the input signal,  $x(t)$ , must oscillate around zero which can be guaranteed by subtracting its mean value  $\langle x \rangle = N^{-1} \sum_{l=1}^N x(l\Delta t)$  with  $\Delta t = 0.25s$ , and (ii) a narrow frequency band which is ensured by incorporating a bandpass frequency filter, e.g., confining frequencies to the HF band (0.15–0.4Hz) in the case of respiration. In practice the Hilbert transform can easily be computed by rewriting Eq. (1) into the product of the Fourier transform of  $1/(\pi t)$ , being  $-i \text{sgn}(f)$  with frequency  $f$ , and the Fourier transform of  $x(t)$  using the convolution theorem. We further denote by  $\varphi_{\text{real resp}}(t)$  the phase signal calculated from thorax excursion by Eq. (2).

### C. Reconstructing Respiration from ECG Data

Our *first* reconstruction method exploits the variation of the axis of the heart caused by respiration and resulting in

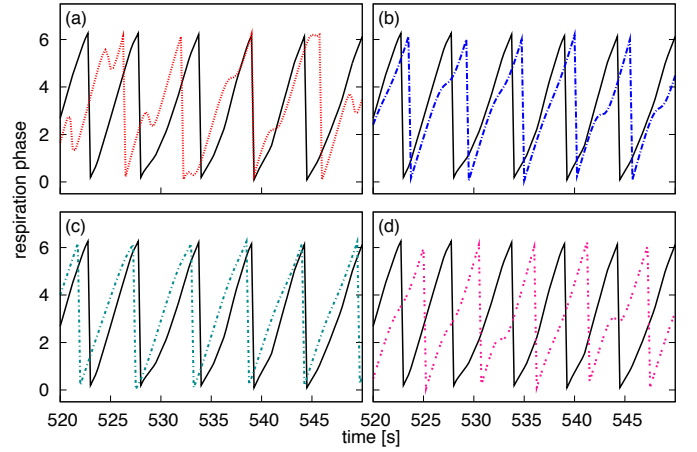


Fig. 2. Comparison of phases for real respiration (black, solid line) and four types of reconstructed respiration (dotted curves, colors correspond to those in Fig. 1) in a randomly chosen subject. (a)–(c) Reconstruction from three orthogonal bipolar ECG-leads after Frank: (a) X, (b) Y, and (c) Z; (d) reconstruction from RR intervals. For the shown fragments the reconstruction based on the Frank-Z lead in (c) performs best, i.e., it results in a relatively stable phase difference between real respiration and reconstructed respiration.

a modulation of R-peak amplitude. This means, the envelope of the raw ECG, using the (resampled) R-peak amplitudes as nodes, can serve as a respiration proxy. We calculate from all three resampled R-peak amplitude signals,  $x^{(j)}(t)$  with  $j = X, Y, Z$  indicating the Frank leads, the instantaneous amplitude functions (reconstructed breathing signals),  $A^{(j)}(t)$ , and the instantaneous phase signals,  $\varphi_{\text{rec resp}}^{(j)}(t)$ . For this we employ Fourier filtering, i. e., transforming the resampled signal to frequency space by a fast Fourier transform (FFT), applying a bandpass filter adjusted to HF components, and transforming back to time space by an inverse FFT. In this paper we explore different cut-off frequencies for the bandpass filter and compare it with a Gaussian filter function. Finally, an analytical signal approach following Eq. (2) yields the reconstructed respiratory phases. Examples of the phases  $\varphi_{\text{rec resp}}^{(X)}(t)$ ,  $\varphi_{\text{rec resp}}^{(Y)}(t)$ , and  $\varphi_{\text{rec resp}}^{(Z)}(t)$  are depicted in Fig. 2(a–c) together with the phase  $\varphi_{\text{real resp}}(t)$  of real respiration.

The *second* reconstruction method exploits the RSA mechanism. Changes in the breathing pattern alter the HF spectral components [33]–[35], and hence, respiratory components can be extracted from a RRI time series by Fourier filtering and an analytical signal approach as described above. Note that the strength of RSA effects varies among subjects and there are subjects where RSA can not be used to extract respiration from heartbeat data, see our paper [21] for an extended discussion. After reconstructing respiration from heartbeat intervals we calculate a phase signal,  $\varphi_{\text{rec resp}}^{(RRI)}(t)$ , according to Eq. 2. Figure 2(d) shows  $\varphi_{\text{rec resp}}^{(RRI)}(t)$  together with  $\varphi_{\text{real resp}}(t)$  for a typical post-infarction patient.

### D. Phase of the Heartbeat-Interval Signal

For heartbeat we define a sawtooth phase signal by considering linear phase increases between R peaks, i.e.  $\varphi_{\text{heartbeat}}(t_k) = 0$  and  $\varphi_{\text{heartbeat}}(t) \rightarrow 2\pi$  ( $t \rightarrow t_{k+1}$ ) for each  $k$ ,

$$\varphi_{\text{heartbeat}}(t) = 2\pi \frac{t - t_k}{t_{k+1} - t_k}, \quad \forall t \text{ with } t_k \leq t < t_{k+1}. \quad (3)$$

### E. Quantifying Phase Synchronization

Two signals are  $n : m$  phase synchronized when their phases fulfill a locking condition ( $\varphi_2$  represents the slow oscillator)

$$\Delta\Psi_{n:m}(t) = m\varphi_1(t) - n\varphi_2(t) \approx \text{const.} \quad (4)$$

for fixed integer values  $n$  and  $m$  and within a certain time interval  $\nu$  given by  $t_\nu \leq t < t_\nu + \Delta\tau$  with  $\Delta\tau > 0$ . A convenient approach to detect phase locking is to consider complex exponentials of the phase differences,  $\Delta\Psi_{n:m}$ , and average them over the time interval  $\Delta\tau$  to obtain the phase-synchronization index  $\gamma_{\nu,n:m}$  for each window  $\nu$ , i. e.,

$$\gamma_{\nu,n:m} = \left| \langle e^{i\Delta\Psi_{n:m}(t)} \rangle_\nu \right|. \quad (5)$$

In the case of perfect phase synchronization in the segment  $\nu$  one obtains  $\gamma_{\nu,n:m} = 1$ , while small  $\gamma_{\nu,n:m}$  are expected for unsynchronized segments. We define the global synchronization index as the mean over all windows,  $\gamma_{n:m} = N_\nu^{-1} \sum_{\nu=1}^{N_\nu} \gamma_{\nu,n:m}$ .

By studying phase locking for real respiration and each of the four reconstructed respiration signals and setting  $n = m = 1$  we can infer which reconstruction method and/or which Frank-lead is suited best for an ECG based respiration proxy. The best reconstruction will result in the largest mean  $\gamma$  which we further denote by  $\gamma_{1:1}^{\text{resp resp}}$ .

Then we study cardio-respiratory phase-synchronization by considering the phase differences  $\Delta\Psi_{n:m} = m\varphi_{\text{heartbeat}} - n\varphi_2$  with  $\varphi_2 = \varphi_{\text{real resp}}^{(X)}, \varphi_{\text{rec resp}}^{(Y)}, \varphi_{\text{rec resp}}^{(Z)}, \varphi_{\text{rec resp}}^{(RRI)}$ , and  $\varphi_{\text{rec resp}}^{(RRI)}$ . We denote the associated phase-synchronization index by  $\gamma_{n:m}^{\text{cardio resp}}$ . To determine an appropriate value of  $n$  for a given  $m$  ( $m = 1$  and  $2$  in this study only), we count the actual number of heartbeats that occur during eight complete respiration cycles and divide by  $8/m$  (integer division).

In all cases we calculate  $\gamma_{\nu,n:m}$  within windows  $\nu$  of 128 data points (4Hz) with an overlap of 96 data points.

### F. Deceleration Capacity

To study changes of cardio-respiratory phase synchronization with the mortality risk of the patients we calculate deceleration capacity (DC) by *phase rectified signal averaging* (PRSA) [11], [12]. In the PRSA algorithm (i) anchors at positions  $\xi$  are selected in the RRI signal ( $x_i$ ) for moderate decelerations ( $x_{\xi-1} < x_\xi < 1.05x_{\xi-1}$ ), and (ii) the surroundings of each anchor are then averaged with respect to the anchor position  $\xi$  to obtain the PRSA signal  $\bar{x}(i)$ . DC is defined by  $\text{DC} = \frac{1}{4}[\bar{x}(0) + \bar{x}(1) - \bar{x}(-1) - \bar{x}(-2)]$ .  $\text{DC} \leq 2.5\text{ms}$  was associated with high mortality risk,  $2.5\text{ms} < \text{DC} \leq 4.5\text{ms}$  with intermediate risk, and  $\text{DC} > 4.5\text{ms}$  with low risk [11].

## III. RESULTS AND DISCUSSION

Figure 3 shows the 1:1 phase-synchronization between real respiration and ECG-based reconstructions, using both R-peak amplitudes [Fig. 3(a)] and the beat-to-beat time intervals [Fig. 3(b)], vs. random phase synchronization; generated by inverting the time of the real respiration signal. For each patient we used the best reconstruction from all three amplitude signals in Fig. 3(a). While there are many patients with

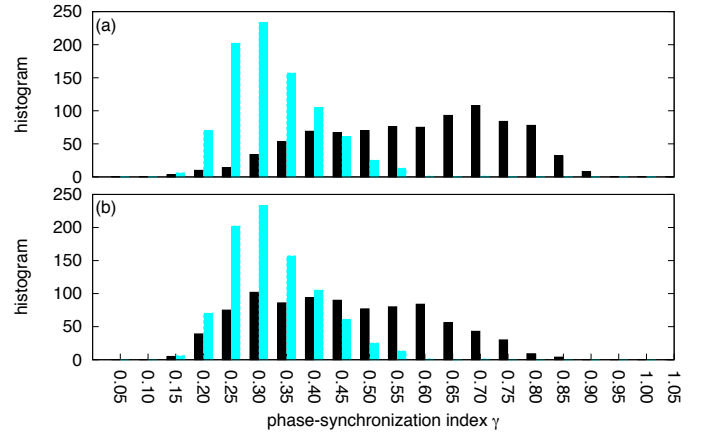


Fig. 3. 1:1 phase-synchronization index  $\gamma_{1:1}^{\text{resp resp}}$  for real and reconstructed respiration (black bars), compared with random phase synchronization (blue bars). Histograms are derived from (a) the best reconstruction from all three R-peak amplitude signals, and (b) the reconstruction from RR-intervals.

good reconstructions from both methods, indicated by large  $\gamma_{1:1}^{\text{resp resp}}$ , there is a clear advantage of R-peak amplitude based reconstruction over RR intervals. Note the bimodal shape in Fig. 3(b) indicating that there are patients whose strong RSA effects allow for a good reconstruction. We suspect that the poorer overall reconstruction capability of the RR-interval method is originated in a reduced RSA in high-risk patients. This is supported by our significance tests concerning the distinguishability of risk classes based on the cardio-respiratory synchronization index (not shown). The mean performance of the breathing reconstruction for both methods and for three different bandpass filters prior the Hilbert transform is reported in Tab. I. Note that a Gaussian filter together with the Frank-Z lead results in the best reconstruction for 39.4% of the patients. Overall the R-peak amplitude method outperforms the RR interval method in 92.6 to 94.9% of all patients.

Our results from studying  $n:1$  and  $n:2$  cardio-respiratory coupling, for each patient using the breathing reconstruction from the method that yields the largest  $\gamma_{1:1}^{\text{resp resp}}$ , are depicted in Fig. 4. We find that the overall cardio-respiratory phase-synchronization is systematically larger for reconstructed breathing. However, the distribution of  $\gamma_{n:m}^{\text{cardio resp}}$  is preserved. We suspect this effect is caused by an ‘additional harmonic denoising’ of the signals due to the methodology.  $\gamma_{n:m}^{\text{cardio resp}}$  does not significantly depend on age except for some decreases in advanced age, see Tab. II. However, it distinguishes all

TABLE I  
AVERAGE PHASE-SYNCHRONIZATION INDEX  $\gamma_{1:1}^{\text{resp resp}}$  SEPARATELY FOR R-PEAK AMPLITUDE AND RR INTERVAL BASED BREATHING RECONSTRUCTION AND FOR THREE FREQUENCY FILTERS. LOWER ROWS INDICATE THE PERCENTAGE OF ALL PATIENTS WHERE THE RESPECTIVE RECONSTRUCTION OUTPERFORMS THE OTHER THREE RECONSTRUCTIONS.

Frequency band (Hz)		R-peak ampl. Frank-X	R-peak ampl. Frank-Y	R-peak ampl. Frank-Z	RR intervals	Mean
		Mean $\gamma$	Mean $\gamma$	Mean $\gamma$	Mean $\gamma$	Mean $\gamma$
0.15-0.40 (HF-band)	Mean $\gamma$	0.480	0.488	0.494	0.423	0.471
	[%]	27.3	32.0	33.3	7.4	N.A.
0.16-0.51	Mean $\gamma$	0.490	0.501	0.507	0.431	0.482
	[%]	25.1	31.7	36.7	6.5	N.A.
$\mu = 0.35$ $\sigma = 0.10$	Mean $\gamma$	0.512	0.521	0.532	0.442	0.502
	[%]	23.0	32.5	39.4	5.1	N.A.

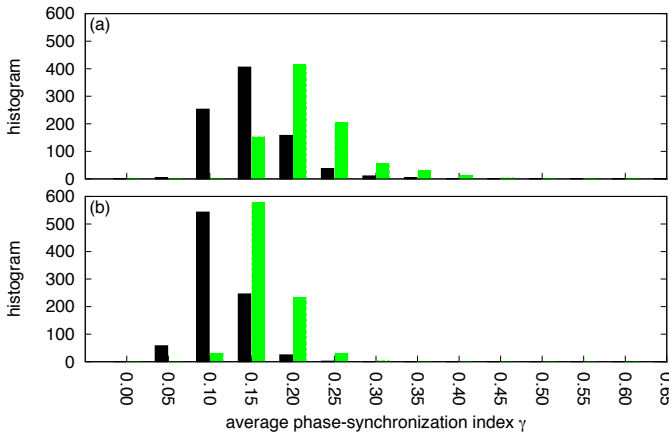


Fig. 4. Histograms of average phase-synchronization index  $\gamma_{n:m}^{\text{cardioresp}}$  for (a)  $n:1$  and (b)  $n:2$  cardio-respiratory phase synchronization, comparing results of real (black bars) and reconstructed (green bars) respiration.

three mortality-risk classes defined by DC successfully and independently of the reconstruction method.

#### IV. CONCLUSION

We have explored two different methods to reconstruct respiration from ECG recordings and found that for a vast majority (approx. 94% depending on the filter parameters) of post-infarction patients a reconstruction based on R-peak amplitude outperforms a reconstruction based on beat-to-beat time intervals. This implies that the cardio-respiratory coupling is rather characterized by peak-amplitude modulations than by frequency modulations (RSA effects). Although, different ECG leads seem to be optimal for a peak amplitude based reconstruction of respiration for different individuals, differences are negligible and multi-lead ECG recordings are only required for applications of needs for high reliability. In cost-efficient ambulant setups and/or long-term Holter-ECG recordings respiration signals of adequate quality can be reconstructed from a single ECG-lead signal. However, this does not render obsolete high-precision measurements of respiration as often required in stationary and/or intense care setups. We are convinced that ECG based reconstruction of breathing is particularly interesting for sports medicine applications or sports instruments used for training purposes where belt measurements are disturbing, e. g., portable monitoring

TABLE II

AGE AND DC DEPENDENCE OF CARDIO-RESPIRATORY PHASE SYNCHRONIZATION FOR REAL RESPIRATION AND ITS RECONSTRUCTION CHARACTERIZED BY THE INDEXES  $\gamma_{n:1}^{\text{CARDIORESP}}$  AND  $\gamma_{n:2}^{\text{CARDIORESP}}$ . PROBABILITIES OF EQUIVALENT MEANS IN EACH SUBGROUP AND THE NEXT SUBGROUP EMPLOYING A T-TEST ARE INDICATED BY SYMBOLS:  $p < 0.001$  ( $\ddagger$ ),  $p < 0.01$  ( $\dagger$ ), AND  $p < 0.03$  (\*). AGES  $\geq 70$ YRS ARE COMPARED WITH  $< 50$ YRS, AND DC  $> 4.5$ MS WITH  $0 < DC \leq 2.5$ MS.

heartbeat vs.	real respiration		best R-peak amplitude		RR interval	
	n:1	n:2	n:1	n:2	n:1	n:2
box-filter [0.16Hz-0.51Hz]						
< 50	0.177	0.128	0.252	0.181	0.213	0.154
age [yrs] 50 – 59	0.176	0.128	0.253	0.180	0.210	0.151
60 – 69	0.168 $\ddagger$	0.125 $\dagger$	0.249	0.178 $\dagger$	0.207	0.152 $\ddagger$
$\geq 70$	0.153 $\ddagger$	0.117 $\ddagger$	0.242	0.169 $\ddagger$	0.201 $\ddagger$	0.144 $\ddagger$
DC [ms]						
0 < DC $\leq 2.5$	0.146 $\ddagger$	0.117	0.226*	0.158 $\ddagger$	0.185 $\ddagger$	0.131 $\ddagger$
2.5 < DC $\leq 4.5$	0.159 $\ddagger$	0.121 $\ddagger$	0.240 $\ddagger$	0.171 $\ddagger$	0.196 $\ddagger$	0.143 $\ddagger$
4.5 < DC < 12	0.181 $\ddagger$	0.130 $\ddagger$	0.263 $\ddagger$	0.189 $\ddagger$	0.219 $\ddagger$	0.160 $\ddagger$

devices used by cyclists, runners, or alpinists to keep track of their own performance or to avoid health threatening events caused by overexertion and overtraining. Moreover, there is an ongoing demand of more portable sleep monitoring systems which can be distributed to a larger group of patients and controls at home enabling statistically more reliable large scale studies.

By using breathing reconstructions we have further investigated cardio-respiratory coupling and found a larger average phase synchronization for the reconstruction compared with real respiration. Our results from comparing phase synchronization to a mortality-risk related index indicate that a reduced cardio-respiratory coupling correlates with high mortality risk. Hence, phase-synchronization might complement established risk scores. However, we also confirmed a relatively short overall duration of synchronous behaviour of heartbeat and respiration (only approx. 5% resulting in small  $\gamma_{n:m}^{\text{cardioresp}}$ ) that we independently observed in sleep data (see conference talk of A.Y.S.). Therefore, recordings longer than 30 minutes are needed to derive actual risk predictors from phase-synchronization analysis. We are currently testing our hypotheses for 24h recordings.

#### ACKNOWLEDGMENT

We acknowledge financial support from the European Union project SOCIONICAL and thank R. Schneider for advice.

#### REFERENCES

- [1] H. V. Huikuri *et al.*, *N. Engl. J. Med.*, **345**(20):1473–1482, 2001.
- [2] A. E. Buxton, *J. Cardiovasc. Electrophysiol.*, **16**(9):S25–S27, 2005.
- [3] R. J. Myerburg *et al.*, *Ann. Intern. Med.*, **119**(12):1187–1197, 1993.
- [4] R. J. Myerburg *et al.*, *Amer. J. Cardiol.*, **80**(Sp. Iss. 5B):F10–F19, 1997.
- [5] Z. J. Zheng *et al.*, *Circulation*, **104**(18):2158–2163, 2001.
- [6] A. J. Moss *et al.*, *N. Engl. J. Med.*, **335**(26):1933–1940, 1996.
- [7] A. J. Moss *et al.*, *N. Engl. J. Med.*, **346**(12):877–883, 2002.
- [8] A. J. Moss, *N. Engl. J. Med.*, **309**(6):331–336, 1983.
- [9] J. Mukharji *et al.*, *Am. J. Cardiol.*, **54**(1):31–36, 1984.
- [10] P. K. Stein and R. E. Kleiger, *Annu. Rev. Med.*, **50**:249–261, 1999.
- [11] A. Bauer *et al.*, *Lancet*, **367**:1674, 2006.
- [12] J. W. Kantelhardt *et al.*, *Chaos*, **17**(1):015112, 2007.
- [13] C. K. Peng *et al.*, *Chaos*, **5**(1):82–87, 1995.
- [14] S. Havlin *et al.*, *Physica A*, **274**(1-2):99–110, 1999.
- [15] T. H. Mäkitallio *et al.*, *Am. J. Cardiol.*, **83**:836–839, 1999.
- [16] H. V. Huikuri *et al.*, *Circulation*, **101**:47–53, 2000.
- [17] H. V. Huikuri *et al.*, *Phil. Trans. R. Soc. A*, **367**:1223–1238, 2009.
- [18] M. Peltola *et al.*, *Ann. Med.*, **40**(5):376–382, 2008.
- [19] D. L. Eckberg, *J. Physiol.*, **548**(2):339–352, 2003.
- [20] F. Yasuma and J. Hayano, *Chest*, **125**(2):683–690, 2004.
- [21] C. Hamann *et al.*, *Chaos*, **19**(1):015106, 2009.
- [22] A. Pikovsky, M. Rosenblum, and J. Kurths. *A universal concept in nonlinear sciences*. Cambridge University Press, 2001.
- [23] M. Paluš, *Phys. Lett. A*, **235**(4):341–351, 1997.
- [24] P. Tass *et al.*, *Phys. Rev. Lett.*, **81**(15):3291–3294, 1998.
- [25] C. Schäfer *et al.*, *Nature*, **392**(6673):239–240, 1998.
- [26] C. Schäfer *et al.*, *Phys. Rev. E*, **60**(1):857–870, 1999.
- [27] E. Toledo *et al.*, *Med. Eng. Phys.*, **24**(1):45–52, 2002.
- [28] R. P. Bartsch *et al.*, *Phys. Rev. Lett.*, **98**(5):054102, 2007.
- [29] M. G. Rosenblum *et al.*, *Handbook of biological physics*. Vol. 4, *Neuroinformatics*, chapter Phase-Synchronization: Form theory to analysis, pages 279–321. Elsevier, Amsterdam, 2001.
- [30] R. Schneider, Opensource QRS detector, [www.librasch.org](http://www.librasch.org), 2005.
- [31] D. Gabor, *Radio Commun. Eng.*, **93**:429, 1946.
- [32] B. Boashash, *Proc. IEEE*, **80**(4):520–538, 1992.
- [33] J. A. Hirsch and B. Bishop, *Am. J. Physiol.*, **241**:H620, 1981.
- [34] T. E. Brown *et al.*, *J. Appl. Physiol.*, **75**:2310, 1993.
- [35] J. Penttilä *et al.*, *Clin. Physiol.*, **21**(3):365–376, 2001.